



HHS Public Access

Author manuscript

Nat Neurosci. Author manuscript; available in PMC 2011 September 01.

Published in final edited form as:

Nat Neurosci. 2011 March ; 14(3): 331–337. doi:10.1038/nn.2754.

Timing of neurogenesis is a determinant of olfactory circuitry

Fumiaki Imamura¹, Albert E. Ayoub^{2,3}, Pasko Rakic^{2,3}, and Charles A. Greer^{1,2}

¹Departments of Neurosurgery, Yale University School of Medicine, 333 Cedar Street, New Haven, CT 06510, USA

²Department of Neurobiology, Yale University School of Medicine, 333 Cedar Street, New Haven, CT 06510, USA

³Department of The Kavli Institute of Neuroscience, Yale University School of Medicine, 333 Cedar Street, New Haven, CT 06510, USA

Abstract

An odorant receptor map in mammals, that is constructed by the glomerular coalescence of sensory neuron axons in the olfactory bulb, is essential for proper odor information processing. However, how this map is linked with olfactory cortex is unknown. Here, we use a battery of methods, including various markers of cell division in combination with tracers of neuronal connections and time-lapse live imaging, to show that early- and late-generated mouse mitral cells become differentially distributed within the dorsal and ventral subdivisions of the odorant receptor map. In addition, we demonstrate that the late-generated mitral cells extend significantly stronger projections to the olfactory tubercle than the early-generated. Together, these data indicate that the odorant receptor map is developmentally linked to the olfactory cortices in part by the birthdate of mitral cells. This endows different olfactory cortical regions a role to process information from distinct regions of odorant receptor map.

Keywords

olfactory bulb; odorant receptor map; olfactory circuits; development; neurogenesis; neurogenetic gradients

The olfactory system, similar to other sensory systems, uses the position of cells within a topographic map to organize and analyze sensory information. Odors detected by olfactory sensory neurons are first relayed to the olfactory bulb glomeruli where the olfactory sensory neuron axons form synapses with the dendrites of projection neurons, the mitral/tufted cells. Because each olfactory sensory neuron expresses only 1 of ~1200 odorant receptors and olfactory sensory neurons having same odorant receptor converge into only 2–3 glomeruli/olfactory bulb^{1–3}, the spatial arrangement of glomeruli on the surface of olfactory bulb

Users may view, print, copy, download and text and data- mine the content in such documents, for the purposes of academic research, subject always to the full Conditions of use: http://www.nature.com/authors/editorial_policies/license.html#terms

Author Contributions F.I. and C.A.G. designed the study, analyzed data, and wrote the manuscript. F.I. conducted the experiments. Time-lapse live imaging was done by F.I. and A.E.A. F.I., C.A.G., A.E.A. and P.R. discussed the results and commented on the manuscript.

establishes an “odorant receptor map”⁴. Olfactory sensory neurons expressing different odorant receptors can also differ in their expression of combinations of molecules that regulate axon fasciculation, convergence, and targeting^{5–9}. Thus, while the afferent innervation of an individual glomerulus is molecularly homogeneous, as a population, glomeruli are highly heterogeneous. Therefore, the odorant receptor map can be divided into several distinct zones or domains based on the constellation of the molecular phenotypes of olfactory sensory neuron axons^{8,10,11}. Finally, the glomeruli activated by odors with similar molecular features are closely positioned, and define clusters in the map^{12–14}.

Mice whose olfactory sensory neurons projecting to dorsal glomeruli are ablated retain the ability to detect odors, but lack fear responses to predator odors¹⁰. This suggests that the olfactory bulb glomeruli in different regions of the odorant receptor map play distinct roles in odor information processing; a concept that is supported by the preservation of odorant receptor maps between the right and left olfactory bulbs in both mice and rats^{15,16}. Despite the functional importance of the odorant receptor map, the rules used to decode the map by the olfactory bulb projection neurons and olfactory cortices are unknown. Direct projection of the odorant receptor map to the olfactory cortex is unlikely; recent *in vivo* studies show that individual odors are sparsely represented in broad regions of piriform cortex, without evidence of clusters^{17,18}. Similar findings were reported in the olfactory system of *Drosophila*¹⁹ and zebrafish²⁰. Finding the rules that link the maps of odorant receptors in olfactory bulb and in the olfactory cortex is critical for understanding anatomical and physiological basis of odor processing in mammals. Previous studies suggested that olfactory cortices receive axons from subpopulations of mitral cells that are non-uniformly distributed throughout the mitral cell layer (MCL); for example, the olfactory tubercle preferentially receives input from mitral cells in the ventral olfactory bulb^{21,22}. However, the relationship between the distribution of mitral cells sending axons to the olfactory tubercle and the odorant receptor map remains unclear.

In the present study, we show that mitral cells having different birthdates are differentially distributed in the dorsomedial and ventrolateral regions in olfactory bulb, which, defined by OCAM expression, are correlated with the dorsal and ventral zones of the odorant receptor map. This finding is reminiscent of the birthdate-dependent dendritic targeting of glomeruli by projection neurons in *Drosophila*²³ as well as the presence of areal and laminar neurogenetic gradients among cytoarchitectonic areas in the mammalian neocortex, including the human and non-human primates^{24,25}. Here we also present data suggesting that the late-generated mitral cells migrate tangentially toward postero-ventro-lateral regions in the olfactory bulb guided by axonal scaffold. Finally, we demonstrate that the olfactory tubercle is preferentially innervated by late-generated mitral cells. These data indicate that mitral cell birthdates may be a determinant of their location in the MCL and indirectly shaping innervation pattern of olfactory cortices.

Results

Mitral cell location and birthdate

To determine mitral cell birthdates we used one of three thymidine analogs (XdU), BrdU, CldU, or IdU, which label cells in the S-phase of the cell cycle. The presence of a population

plug defined embryonic day (E) 0; XdU injections were at E9, 10, 11, 12, or 13. Pups were sacrificed at postnatal day (P) 20, and XdU-labeling of mitral cells was immunohistochemically analyzed with XdU and Tbx21 antibodies. Approximately 1, 18, 28, 12, and 6% of mitral cells were labeled with XdU injected at E9, 10, 11, 12, and 13, respectively (Fig. 1a). XdU+ cells, some of which were Tbx21+, were also seen in the external plexiform layer and glomerular layer. Therefore, these cells are most likely tufted cells (Tbx21+) and periglomerular cells (Tbx21-) that are generated shortly after mitral cells with some temporal overlap^{26,27}. In addition, XdU+ but Tbx21- cells were found in the MCL, especially following XdU injections at later time points (arrows in Fig. 1g). These are most likely a subtype of granule cell which is located in the MCL and generated as early as E12.5^{27,28}.

The majority of E10-generated mitral cells were located in the dorsomedial MCL, and fewer in the lateral MCL (Fig. 1b–d). In contrast, E12-generated mitral cells localized to the ventrolateral region (Fig. 1e–g). This recalled the dorsal and ventral zone subdivision of the odorant receptor map defined by OCAM expression²⁹. Therefore, we subdivided the entire MCL in a coronal slice into dorsomedial (D-MCL) and ventrolateral (V-MCL) regions based on glomerular OCAM expression (Fig. 1h). To quantify the distribution of XdU labeled mitral cells, the percentages in each subdivision were calculated using five coronal slices taken every 400µm from the anterior to the posterior olfactory bulb (Fig. 1i and Supplementary Fig. 1a). Comparing the results acquired from the same olfactory bulb, we found that the percentage of E10-generated mitral cells was always higher in D- than V-MCL ($p=0.002$), while more E12-generated mitral cells were in the V-MCL ($p=0.002$) (Fig. 1j). MCL maps superimposed with E10- and E12-generated mitral cells revealed the higher density of E10-generated mitral cells in D- than V-MCL, while E12-generated mitral cells were denser in V-MCL (Supplementary Fig. 1b). The distributions of E9-generated and E13-generated mitral cells were similar to those of E10-generated and E12-generated mitral cells, respectively. There was no significant difference in the D- and V-MCL distribution of E11-generated mitral cells ($p=0.563$) (Fig. 1j). These results clearly show that early- and late-generated mitral cells are differentially distributed in the D- and V-MCLs.

Furthermore, we confirmed that the differential distribution of E10-, E11-, and E12-generated mitral cells we have shown in the P20 olfactory bulb, is already present at P0 (Supplementary Fig. 2). Indeed at P0, higher percentages of E10-generated mitral cells were found in D- than V-MCLs ($p=0.008$), whereas more E12-generated mitral cells were found in V- than D-MCLs ($p=0.008$). No significant difference was seen in the distribution of E11-generated mitral cells ($p=0.156$).

Integration of mitral cells into developing olfactory bulb

A possible mechanism to establish the distinct birthdate-dependent distribution of mitral cells in the MCL is an overproduction and subsequent cell death in specific regions. To test this hypothesis, we first examined if mitral cells die during embryogenesis. We chose E11-generated cells to examine mitral cell death because our results showed XdU injections at E11 resulted in the largest number of labeled mitral cells (Fig. 1a). Under these conditions, optimized for detecting mitral cell death by double labeling for cleaved-caspase3 and BrdU,

we found no evidence of cell death among E11-generated cells, including mitral cells (Supplementary Fig. 3). Moreover, at most only a few cleaved-caspase3 positive cells, with or without BrdU labeling, were found in olfactory bulb slices at any of the ages examined: E11, E12, E13, E14, E15, and E17. The same results were obtained when we assayed cell death with an alternative method, a TUNEL assay (Supplementary Fig. 4). These results strongly suggest that mitral cells do not die during embryogenesis. Therefore, regardless of their time of origin, cell death is not a determinant of the final localization of mitral cells in the MCL.

An alternative hypothesis is that early- and late-generated mitral cells are fated to integrate specifically into the dorsomedial and ventrolateral portions of the olfactory bulb, respectively. Therefore, we examined the distribution of E10-, E11-, and E12-generated mitral cells at E15 (Fig. 2a). *Tbr1* was used to identify mitral cells since not all express *Tbx21* at E15. Most E10-generated mitral cells reached the nascent MCL by E15 (Fig. 2b). To quantify their distribution, the olfactory bulb was radially divided into twelve compartments and the percentages of *XdU+*/*Tbr1+* cells in each compartment were calculated (Fig. 2d). Unexpectedly, E10-generated mitral cells were evenly distributed throughout the olfactory bulb, rather than preferentially in the dorsomedial portion (Fig. 2e). In contrast, larger numbers of E12-generated mitral cells was found in ventrolateral portion, although most were in the intermediate zone between the nascent MCL and ventricular zone (Fig. 2c,g). E11-generated mitral cells showed a distribution pattern intermediate between E10- and E12-generated cells (Fig. 2f). A Rayleigh test revealed that E10-generated mitral cells were uniformly distributed in the olfactory bulb at E15 ($p=0.258$). However, the distributions of E11- and E12-generated mitral cells were non-uniform ($p<0.001$ for both E11 and E12-generated mitral cells). The distribution peak of both E11- and E12-generated mitral cells were within the ventrolateral portion of the olfactory bulb. These results suggest that late-generated mitral cells preferentially integrate into the ventrolateral portion of the olfactory bulb, while early-generated mitral cells do not exhibit a preferential topographic integration. Therefore, the sparse density of E10-generated mitral cells in V-MCL may be attributed to the integration of larger numbers of E11- and E12-generated mitral cells. Likewise, the equal distribution of E11-generated mitral cells in D- and V-MCL found in P20 and P0 olfactory bulbs may reflect the integration of larger numbers of E12-generated mitral cells into V-MCL during continuing embryogenesis.

Tangential migration of mitral cells

What is the underlying mechanism for the specific targeting of late-generated mitral cells to the V-MCL of olfactory bulb? Because mitral cell precursors are first generated in the ventricular zone of the presumptive olfactory bulb³⁰, we examined whether more mitral cells are generated in the ventrolateral ventricular zone. To test this, E12-generated cells were labeled with BrdU, and their distributions were examined at E13 and E14. At E13 most BrdU+ cells were found in the ventricular zone (Fig. 3a); the nuclei of these cells were radially elongated and parallel to the processes of radial glia (RC2+) (Fig. 3b), suggesting they were migrating radially from the ventricular zone toward the intermediate zone. However, a preferential distribution in the ventrolateral portion was not detected. The distribution was quantified as described above, but all BrdU+ cells in the olfactory bulb

were included because it was too early to use *Tbr1* expression to identify the E12-generated mitral cells. Despite the non-uniform distribution of E12-generated cells in E13 olfactory bulb ($p < 0.001$), their distribution peak was in the dorsolateral portion (Fig. 3c). At E14, many BrdU+ cells with tangentially elongated nuclei were found in the intermediate zone (Fig. 3d,e). The distribution peak of E12-generated cells in the olfactory bulb also shifted from dorsolateral to lateral (Fig. 3f). Moreover, when the distributions of E12-generated cells were separately analyzed in the anterior and posterior regions of E13 and E14 olfactory bulbs, the percentage of cells found in the ventrolateral portion was higher in the posterior than anterior (Supplementary Fig. 5). From these observations, we propose a hypothesis that E12-generated cells migrate tangentially in the intermediate zone toward the postero-ventrolateral region of the olfactory bulb. It was noted previously from Golgi-stained and DiI-labeled tissues that mitral cells in the intermediate zone have a tangential-like morphology³⁰, but their organization and the underlying reason for the change from radial to tangential was unknown. We suggest that tangentially elongated cells within the intermediate zone are migrating late-generated mitral cells.

To confirm a migratory phenotype in E12-generated mitral cells, we used DCX-GFP mice in which GFP is expressed under the promoter of doublecortin (DCX), a microtubule-associated protein expressed in migrating neurons. After labeling the E12-generated cells with BrdU in the DCX-GFP mice, GFP expression by *Tbr1*+ and/or BrdU+ cells in the E14 olfactory bulb was examined. At this age, GFP+ cells were found at the surface of olfactory bulb including the intermediate zone and MCL; cells in the ventricular zone were weakly GFP+ (Fig. 3g). Most GFP+ cells in the intermediate zone had a tangentially elongated morphology, and both *Tbr1*+ and BrdU+ cells in this region were GFP+ (Fig. 3h). We also found many GFP+/BrdU+/*Tbr1*+ cells (Fig. 3h, asterisks) although not all BrdU+ cells were *Tbr1*+, and vice versa.

To acquire direct evidence of tangential migration in the developing olfactory bulb, we next performed time-lapse imaging. Preparing acute slices from the olfactory bulbs of E14 DCX-GFP embryos, GFP+ cells in the intermediate zones were imaged every 10 minutes. We observed many cells migrating tangentially in the intermediate zone. Although migration was not unidirectional, there were cells migrating toward the posterior portion of the olfactory bulb (Fig. 3i and Supplementary Video 1). Following the migration assay, some tangentially migrating cells were confirmed as mitral cells using *Tbr1*+ immunohistochemistry (Fig. 3j). Consistent with our hypothesis, we also found examples of GFP+ cells that migrated radially (Supplementary Video 2) and GFP+ cells that changed orientation from a radial to tangential in the E15 olfactory bulb (Supplementary Video 3). These results support our hypothesis of the tangential migration of late-generated mitral cells in the intermediate zone of the developing olfactory bulb.

Axons form migratory scaffold for mitral cells

Radial glial processes support radial migration of mitral cells in the ventricular zone (Fig. 3b). However, it is not known what structure, if any, supports tangential migration. Radial glia also have short branches in the intermediate zone of developing olfactory bulb³¹, but it is unlikely that these processes are used for tangential migration; we did not find any

evidence of radial glial processes extending tangentially and contacting E12-generated cells within the intermediate zone of the E14 olfactory bulb (Figs. 3e and 4a,b). It is possible that these short processes are used for changing migration direction from radial to tangential, but not for sustained tangential migration.

An alternative candidate for mediating tangential migration of late-generated mitral cells is the scaffold formed by the axons of early-generated mitral cells. OCAM is expressed early in developing mitral cells and their axons^{32,33}. Therefore, to test for apposition of migrating E12-generated cells and mitral cell axons, we injected BrdU at E12 and stained for OCAM at E14. Mitral cell axons running toward lateral and posterior portions in the intermediate zone were evident in both coronal (Fig. 4c) and horizontal sections (Fig. 4e). The tangentially elongated E12-generated cells were positioned in parallel with, and closely apposed to, the OCAM+ axons (Fig. 4d,f). As a further test, we labeled the axons with DiI injections into the lateral olfactory tract and labeled the nuclei of mitral cells with Tbr1 staining at E15. Consistently, the tangentially elongated mitral cells (Tbr1+) were closely aligned with DiI+ axons of earlier-generated mitral cells (Fig. 4g). We then used immunoelectron microscopy to determine if the Tbr1+ cells were in direct contact with axons. At E15 mitral cells, Tbr1+ cells, were identified by the electron dense DAB reaction in their nuclei and their elongated tangential morphology in horizontal sections. These cells were typically surrounded by many axons (Fig. 4h,i); many of which formed somato-axonal appositions (Fig. 4j; arrowheads).

We observed tangentially elongated BrdU+ and Tbr1+ cells in the intermediate zone only at E14 and E15. At these time points, the axons of early-born mitral cells are most likely the only fibrous structure in this region³⁴, other than the short branches of radial glia. An alternative mechanism for mitral cell migration is the chain migration that is used by olfactory interneurons in the rostral migratory stream. However, we think this is unlikely because we did not observe the dense packing typical of the chain migration characteristic of the rostral migratory stream³⁵. Thus, the axons of early-generated mitral cells are the most plausible structure which can provide a scaffold to support the tangential migration of late-generated mitral cells toward the postero-ventro-lateral portion in the developing olfactory bulb. This adds further support to our initial finding of the differential distribution of early-versus late-generated mitral cells in the olfactory bulb, and is consistent with prior reports that the lateral olfactory tract is first formed by mitral cells in the medial olfactory bulb³⁶.

Differential mitral cell projection to olfactory tubercle

The olfactory tubercle was previously suggested to receive more axons from mitral cells in the ventral olfactory bulb^{21,22}. Here, we injected DiI into the P5 olfactory tubercle and examined the distribution of labeled mitral cells in the olfactory bulb (Fig. 5a). Although labeled mitral cells were found throughout the MCL, consistent with the prior studies, larger numbers of DiI+ mitral cells were found in the ventrolateral region (Fig. 5a). In addition, DiI staining in the external plexiform layer, where the secondary dendrites of mitral cells extend, was most intense in the ventrolateral (Fig. 5c) compared to dorsomedial olfactory bulb (Fig. 5b). For comparison with the odorant receptor map, the MCL was subdivided into D- and V-MCLs, based on glomerular OCAM expression, and the percentages of DiI+ mitral cells

were quantified (Fig. 5d). Because DiI volumes and injection sites in the olfactory tubercle varied between animals, the percentages were variable. Nevertheless, the density of olfactory tubercle projecting mitral cell was significantly heavier in V- than D-MCL ($p=0.002$).

Since the distribution pattern of olfactory tubercle projecting mitral cells in the MCL was similar to that of E12-generated mitral cells, we next examined whether mitral cells with different birthdates differ in their axonal projections to the olfactory tubercle. For this study, another thymidine analog, 5-ethynyl-2'-deoxyuridine (EdU), was used to label mitral cells because EdU detection is compatible with DiI³⁷ (Fig. 5e). Following EdU injection at E10, E11, or E12, DiI was placed into the olfactory tubercle at P5 and the percentages of DiI and EdU double-labeled mitral cells was determined (Fig. 5f). A significantly higher percentage of DiI+ mitral cells were co-labeled with EdU injected at E12 compared to E10 ($p<0.001$) or E11 ($p<0.05$). Thus, the olfactory tubercle receives a heavier axonal projection from late-generated than early-generated mitral cells. This indicates that the asymmetrical distribution of mitral cells innervating the olfactory tubercle is dependent on their birthdates.

Discussion

In the mammalian neocortex the laminar and areal positions of pyramidal neurons, which ultimately determine their connectivity and function, are directly correlated with the time of their origin^{24, 25}. In contrast to the cortical multilayer cellular organization, mitral cells in the olfactory bulb are aligned in single layer, and had not been previously evaluated for segregation into subpopulations based on the timing of their last cell division. Here, we demonstrate that mitral cells having different birthdates are differentially distributed in the MCL, and moreover, that the late-generated mitral cells extend stronger projections to the olfactory tubercle than the early-generated. Our data suggest that, like cerebral cortex²⁴, the birthdates of mitral cells in the olfactory system may be a determinant of their segregation into spatially and functionally defined subpopulations. Thus, we propose the existence of two topographically defined maps in the olfactory bulb which interface at the glomeruli. Map #1 (odorant receptor map) is the glomerular distribution of olfactory sensory neuron axons based on odorant receptor expression. Map #2 (mitral cell map) is the birthdate-dependent location of the mitral cells in the olfactory bulb. Considering the zonal segregation of the odorant receptor map²⁹ and the columnar structure constructed by granule cells in the olfactory bulb³⁸, the formation of the mitral cell map may provide a fundamental framework by which mitral cells decode the signal from olfactory sensory neurons.

Development of the olfactory bulb

The time-course of development is not uniform throughout the olfactory bulb. For example, glomeruli are reported to appear first in the antero-dorsal region of developing olfactory bulb³⁹, although synaptogenesis in the glomerular layer occurred earlier in ventral region⁴⁰. More recently, it was shown that all cells expressing Pcdh21, a mitral cell marker, at E14 were positive for OCAM⁴¹. Among mitral cells, OCAM is expressed only by those in the dorsomedial region of the olfactory bulb³³, indicating that mitral cells in dorsomedial region mature earlier than other mitral cells. Thus, olfactory bulb development may begin

dorsomedially and then expand to the ventrolateral domain of the olfactory bulb. Our results demonstrating a differential distribution of early- and late-generated mitral cells in D- and V-MCLs also supports this perspective, although the segregation was not exclusive. Here, we also propose a plausible hypothesis that a tangential migration of late-generated mitral cells along a scaffold of axons from early-generated mitral cells is an underlying cellular mechanism for dorsomedial–ventrolateral gradient of mitral cell development (Supplementary Fig. 6). Elucidating the molecular mechanisms regulating migration and detachment of migrating mitral cells from the axonal scaffold in the posterior olfactory bulb will give us better insight into spatial and temporal differences in olfactory bulb development.

Mitral cell location, projection, and birthdates

Significant differences in the distribution of E10- and E12-generated mitral cells were found when the MCL was subdivided into dorsomedial and ventrolateral regions, based on glomerular OCAM expression. Because olfactory sensory neurons targeting the dorsal and ventral zones make synapses primarily with mitral cells in the D- and V-MCLs, respectively, odor information from dorsal zone olfactory sensory neurons is processed largely by early-generated mitral cells, while late-generated mitral cells process odor information from ventral zone olfactory sensory neurons. The segregation of early- and late-generated mitral cells into D- and V-MCLs is not an all-or-none event. In both domains early- and late-generated cells are slightly intermingled. While this provides both early- and late-generated mitral cells with an opportunity to process odor information from dorsal and ventral zone olfactory sensory neurons, the ratios are profoundly different. Thus, the distinct location of mitral cells having different birthdates may contribute to a functional specificity to the different zones of the odorant receptor map¹⁰.

In addition, we have demonstrated here that the olfactory tubercle receives a larger number of axons from the E12-generated mitral cells than from those generated at E10 or E11. In rabbits, approximately one-fourth of the mitral cells in the ventral olfactory bulb send their axons to the olfactory tubercle⁴². Our data suggest that the axonal projection of mitral cell to the olfactory tubercle is partly determined by its birthdate. A similar correlation has been observed during genesis of tufted cells, which are born later than mitral cells²⁶ and project predominately to the olfactory tubercle^{21, 43, 44}. Moreover, we propose that mitral cells generated at different time points send their axons to spatially distinct regions in the olfactory cortex. Since early- and late-generated mitral cells send their axons through different sub-laminae in the lateral olfactory tract³², mitral cell axons that target different regions of the olfactory cortices may begin to segregate in lateral olfactory tract. Together with the studies of molecular mechanisms regulating organization of the lateral olfactory tract and axonal topography in olfactory cortices^{45–47}, rules that link the olfactory bulb and the olfactory cortices may be revealed by focusing on birthdates of mitral/tufted cells.

In summary, our studies reveal that both the locations of mitral cell somata in the MCL and the extent of their axonal projections in the olfactory cortices are in part a function of their date of birth. Considering that the spatial distribution of mitral cells with different birthdates correlates systematically with the dorsal and ventral zones of the odorant receptor map, it is

likely that processing of distinct odors in the olfactory cortices depends on the information flow from the dorsal and ventral zones of the odorant receptor map. Thus, our data suggest a developmental mechanism that may be used by the olfactory bulb projection neurons to organize the transmission of information from the odorant receptor map to the olfactory cortices. The physiological significance of an odorant receptor map for information processing in the olfactory cortices is still largely unknown. Also, our data show that while there is a significant difference in cortical projection based on date of birth, it is not exclusive pattern of projections; there is evidence for some intermingling of early- and late-generated mitral cells. Nevertheless, our data establish a developmental gradient in mitral cell location and connections, characteristics that will be useful and we continue to unravel the rules that regulate the odor processing.

Supplementary Material

Refer to Web version on PubMed Central for supplementary material.

Acknowledgments

We thank Dr. Kensaku Mori for the anti-OCAM antibody; Dr. Yoshihiro Yoshihara for the anti-Tbx21 antibody; and Dr. Angelique Bordey for the DCX-GFP mice. The anti-RC2 antibody developed by Dr. M. Yamamoto was obtained from the Developmental Studies Hybridoma Bank developed under the auspices of the NICHD and maintained by The University of Iowa, Department of Biology, Iowa City, IA 52242. We also thank all the members in C. Greer, P. Rakic, and H. Treloar laboratories for technical assistance and discussion. This work is supported by the National Institute of Health and the Kavli Institute for Neuroscience at Yale.

References

1. Vassar R, et al. Topographic organization of sensory projections to the olfactory bulb. *Cell*. 1994; 79:981–991. [PubMed: 8001145]
2. Ressler KJ, Sullivan SL, Buck LB. Information coding in the olfactory system: evidence for a stereotyped and highly organized epitope map in the olfactory bulb. *Cell*. 1994; 79:1245–1255. [PubMed: 7528109]
3. Mombaerts P, et al. Visualizing an olfactory sensory map. *Cell*. 1996; 87:675–686. [PubMed: 8929536]
4. Mori K, Nagao H, Yoshihara Y. The olfactory bulb: coding and processing of odor molecule information. *Science*. 1999; 286:711–715. [PubMed: 10531048]
5. Imai T, Sakano H. Odorant receptor-mediated signaling in the mouse. *Curr Opin Neurobiol*. 2008; 18:251–260. [PubMed: 18721880]
6. Kaneko-Goto T, Yoshihara S, Miyazaki H, Yoshihara Y. BIG-2 mediates olfactory axon convergence to target glomeruli. *Neuron*. 2008; 57:834–846. [PubMed: 18367085]
7. Serizawa S, et al. A neuronal identity code for the odorant receptor-specific and activity-dependent axon sorting. *Cell*. 2006; 127:1057–1069. [PubMed: 17129788]
8. Imai T, et al. Pre-target axon sorting establishes the neural map topography. *Science*. 2009; 325:585–590. [PubMed: 19589963]
9. Imai T, Suzuki M, Sakano H. Odorant receptor-derived cAMP signals direct axonal targeting. *Science*. 2006; 314:657–661. [PubMed: 16990513]
10. Kobayakawa K, et al. Innate versus learned odour processing in the mouse olfactory bulb. *Nature*. 2007; 450:503–508. [PubMed: 17989651]
11. Bozza T, et al. Mapping of class I and class II odorant receptors to glomerular domains by two distinct types of olfactory sensory neurons in the mouse. *Neuron*. 2009; 61:220–233. [PubMed: 19186165]

12. Mori K, Takahashi YK, Igarashi KM, Yamaguchi M. Maps of odorant molecular features in the Mammalian olfactory bulb. *Physiol Rev.* 2006; 86:409–433. [PubMed: 16601265]
13. Johnson BA, Leon M. Chemotopic odorant coding in a mammalian olfactory system. *J Comp Neurol.* 2007; 503:1–34. [PubMed: 17480025]
14. Matsumoto H, et al. Spatial arrangement of glomerular molecular-feature clusters in the odorant-receptor class domains of the mouse olfactory bulb. *J Neurophysiol.* 2010; 103:3490–3500. [PubMed: 20393058]
15. Soucy ER, Albeanu DF, Fantana AL, Murthy VN, Meister M. Precision and diversity in an odor map on the olfactory bulb. *Nat Neurosci.* 2009; 12:210–220. [PubMed: 19151709]
16. Johnson BA, Xu Z, Ali SS, Leon M. Spatial representations of odorants in olfactory bulbs of rats and mice: Similarities and differences in chemotopic organization. *J Comp Neurol.* 2009; 514:658–673. [PubMed: 19363812]
17. Poo C, Isaacson JS. Odor representations in olfactory cortex: “sparse” coding, global inhibition, and oscillations. *Neuron.* 2009; 62:850–861. [PubMed: 19555653]
18. Stettler DD, Axel R. Representations of odor in the piriform cortex. *Neuron.* 2009; 63:854–864. [PubMed: 19778513]
19. Murthy M, Fiete I, Laurent G. Testing odor response stereotypy in the *Drosophila* mushroom body. *Neuron.* 2008; 59:1009–1023. [PubMed: 18817738]
20. Miyasaka N, et al. From the olfactory bulb to higher brain centers: genetic visualization of secondary olfactory pathways in zebrafish. *J Neurosci.* 2009; 29:4756–4767. [PubMed: 19369545]
21. Scott JW, McBride RL, Schneider SP. The organization of projections from the olfactory bulb to the piriform cortex and olfactory tubercle in the rat. *J Comp Neurol.* 1980; 194:519–534. [PubMed: 7451680]
22. Haberly LB, Price JL. The axonal projection patterns of the mitral and tufted cells of the olfactory bulb in the rat. *Brain Res.* 1977; 129:152–157. [PubMed: 68803]
23. Jefferis GS, Marin EC, Stocker RF, Luo L. Target neuron prespecification in the olfactory map of *Drosophila*. *Nature.* 2001; 414:204–208. [PubMed: 11719930]
24. Rakic P, Ayoub AE, Breunig JJ, Dominguez MH. Decision by division: making cortical maps. *Trends Neurosci.* 2009; 32:291–301. [PubMed: 19380167]
25. Molyneaux BJ, Arlotta P, Menezes JR, Macklis JD. Neuronal subtype specification in the cerebral cortex. *Nat Rev Neurosci.* 2007; 8:427–437. [PubMed: 17514196]
26. Hinds JW. Autoradiographic study of histogenesis in the mouse olfactory bulb. I. Time of origin of neurons and neuroglia. *J Comp Neurol.* 1968; 134:287–304. [PubMed: 5721256]
27. Batista-Brito R, Close J, Machold R, Fishell G. The distinct temporal origins of olfactory bulb interneuron subtypes. *J Neurosci.* 2008; 28:3966–3975. [PubMed: 18400896]
28. Imamura F, et al. A leucine-rich repeat membrane protein, 5T4, is expressed by a subtype of granule cells with dendritic arbors in specific strata of the mouse olfactory bulb. *J Comp Neurol.* 2006; 495:754–768. [PubMed: 16506198]
29. Mori K, von Campenhouse H, Yoshihara Y. Zonal organization of the mammalian main and accessory olfactory systems. *Philos Trans R Soc Lond B Biol Sci.* 2000; 355:1801–1812. [PubMed: 11205342]
30. Blanchart A, De Carlos JA, Lopez-Mascaraque L. Time frame of mitral cell development in the mice olfactory bulb. *J Comp Neurol.* 2006; 496:529–543. [PubMed: 16572431]
31. Puche AC, Shipley MT. Radial glia development in the mouse olfactory bulb. *J Comp Neurol.* 2001; 434:1–12. [PubMed: 11329125]
32. Inaki K, Nishimura S, Nakashiba T, Itohara S, Yoshihara Y. Laminar organization of the developing lateral olfactory tract revealed by differential expression of cell recognition molecules. *J Comp Neurol.* 2004; 479:243–256. [PubMed: 15457507]
33. Treloar HB, Gabeau D, Yoshihara Y, Mori K, Greer CA. Inverse expression of olfactory cell adhesion molecule in a subset of olfactory axons and a subset of mitral/tufted cells in the developing rat main olfactory bulb. *J Comp Neurol.* 2003; 458:389–403. [PubMed: 12619073]
34. Hinds JW. Early neuron differentiation in the mouse olfactory bulb. II. Electron microscopy. *J Comp Neurol.* 1972; 146:253–276. [PubMed: 4116342]

35. Lois C, Garcia-Verdugo JM, Alvarez-Buylla A. Chain migration of neuronal precursors. *Science*. 1996; 271:978–981. [PubMed: 8584933]
36. Grafe MR, Leonard CM. Developmental changes in the topographical distribution of cells contributing to the lateral olfactory tract. *Brain Res*. 1982; 255:387–400. [PubMed: 7066696]
37. Salic A, Mitchison TJ. A chemical method for fast and sensitive detection of DNA synthesis in vivo. *Proc Natl Acad Sci U S A*. 2008; 105:2415–2420. [PubMed: 18272492]
38. Willhite DC, et al. Viral tracing identifies distributed columnar organization in the olfactory bulb. *Proc Natl Acad Sci U S A*. 2006; 103:12592–12597. [PubMed: 16895993]
39. Bailey MS, Puche AC, Shipley MT. Development of the olfactory bulb: evidence for glia-neuron interactions in glomerular formation. *J Comp Neurol*. 1999; 415:423–448. [PubMed: 10570454]
40. Blanchart A, Romaguera M, Garcia-Verdugo JM, de Carlos JA, Lopez-Mascaraque L. Synaptogenesis in the mouse olfactory bulb during glomerulus development. *Eur J Neurosci*. 2008; 27:2838–2846. [PubMed: 18588529]
41. Takeuchi H, et al. Sequential arrival and graded secretion of Sema3F by olfactory neuron axons specify map topography at the bulb. *Cell*. 2010; 141:1056–1067. [PubMed: 20550939]
42. Ojima H, Mori K, Kishi K. The trajectory of mitral cell axons in the rabbit olfactory cortex revealed by intracellular HRP injection. *J Comp Neurol*. 1984; 230:77–87. [PubMed: 6096415]
43. Scott JW. Electrophysiological identification of mitral and tufted cells and distributions of their axons in olfactory system of the rat. *J Neurophysiol*. 1981; 46:918–931. [PubMed: 6271931]
44. Nagayama S, et al. Differential axonal projection of mitral and tufted cells in the mouse main olfactory system. *Front Neural Circuits*. 2010; 4
45. Hirata T, Fujisawa H. Environmental control of collateral branching and target invasion of mitral cell axons during development. *J Neurobiol*. 1999; 38:93–104. [PubMed: 10027565]
46. Fouquet C, et al. Robo1 and robo2 control the development of the lateral olfactory tract. *J Neurosci*. 2007; 27:3037–3045. [PubMed: 17360927]
47. Soussi-Yanicostas N, et al. Anosmin-1, defective in the X-linked form of Kallmann syndrome, promotes axonal branch formation from olfactory bulb output neurons. *Cell*. 2002; 109:217–228. [PubMed: 12007408]
48. Yamaguchi M, Mori K. Critical period for sensory experience-dependent survival of newly generated granule cells in the adult mouse olfactory bulb. *Proc Natl Acad Sci U S A*. 2005; 102:9697–9702. [PubMed: 15976032]
49. Burns KA, et al. Nestin-CreER mice reveal DNA synthesis by nonapoptotic neurons following cerebral ischemia hypoxia. *Cereb Cortex*. 2007; 17:2585–2592. [PubMed: 17259645]

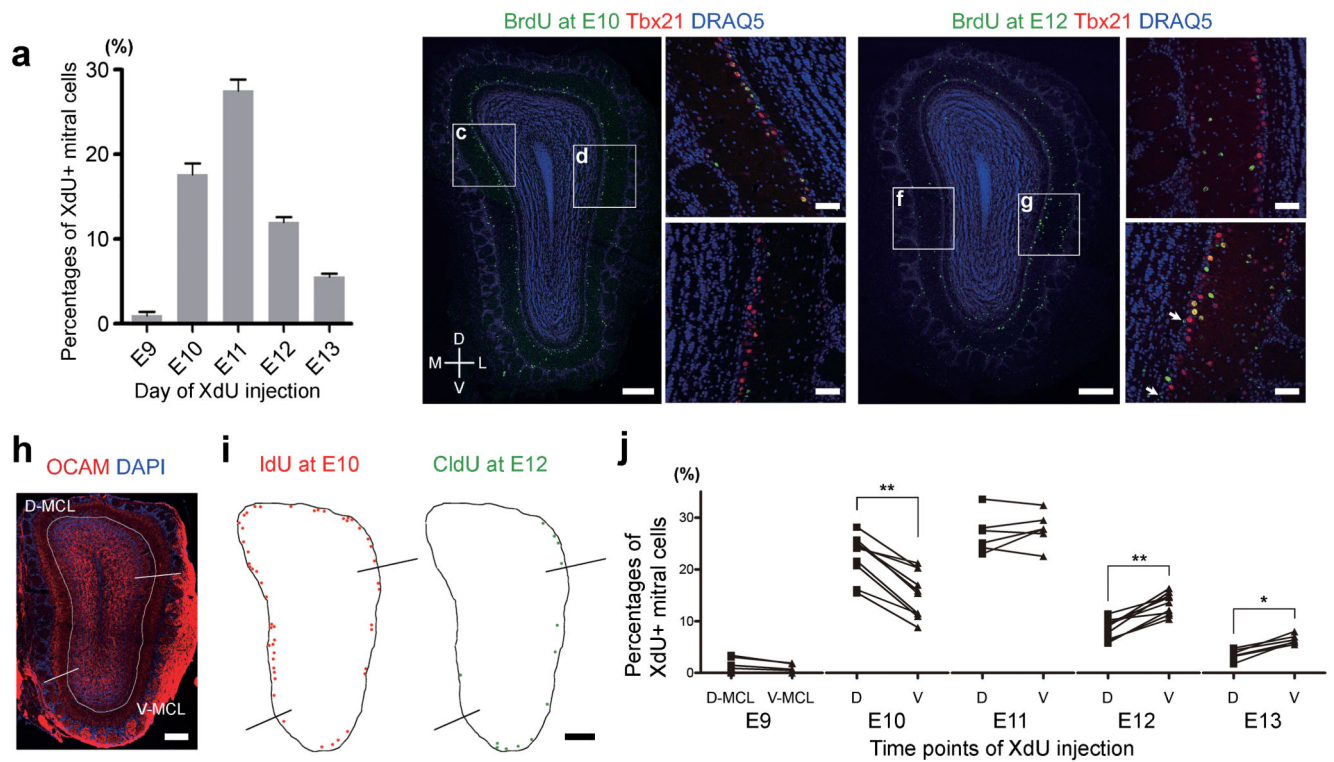


Figure 1.

Distributions of mitral cells with different birthdates in the olfactory bulb.

(a) Percentages of mitral cells in P20 olfactory bulb labeled with thymidine analogs (BrdU, CldU, or IdU) injected at indicated time points. (b–g) Coronal sections of olfactory bulb immunostained with BrdU that were injected into pregnant dams at E10 (b) and E12 (e), respectively. More E10-generated (BrdU+; green) mitral cells (Tbx21+; red) are found in the medial (c) than lateral side (d), while E12-generated mitral cells are preferentially located in the lateral side (f,g). Arrows in (g) indicate the BrdU+ but Tbx21- cells in the MCL. All cell nuclei are stained with DRAQ5 (blue). (h) The MCL was subdivided into dorsomedial (D-) and ventrolateral (V-) MCLs based on the OCAM expression in glomerular layer (red). (i) The representative images showing the position of E10- (red) and E12-generated mitral cells (green) labeled with IdU and CldU, respectively, in an olfactory bulb section. (j) Percentages of thymidine analog-labeled mitral cells found in D- and V-MCLs. Thymidine analogs were applied at indicated time points. Each data point represents a single olfactory bulb, and data obtained from the same olfactory bulb are connected with lines. Significant distribution differences between D- and V-MCLs are found in E10- (** $p=0.002$; $n=10$ olfactory bulbs), E12- (** $p=0.002$; $n=10$), and E13-generated mitral cells (* $p=0.031$; $n=6$), but not in E9- ($p=0.125$; $n=6$) or E11-generated mitral cells ($p=0.563$; $n=6$) (Wilcoxon signed rank test). Error bars represent s.e.m. Scale bars represent 200 μ m (b, e, h, i) and 50 μ m (c,d,f,g).

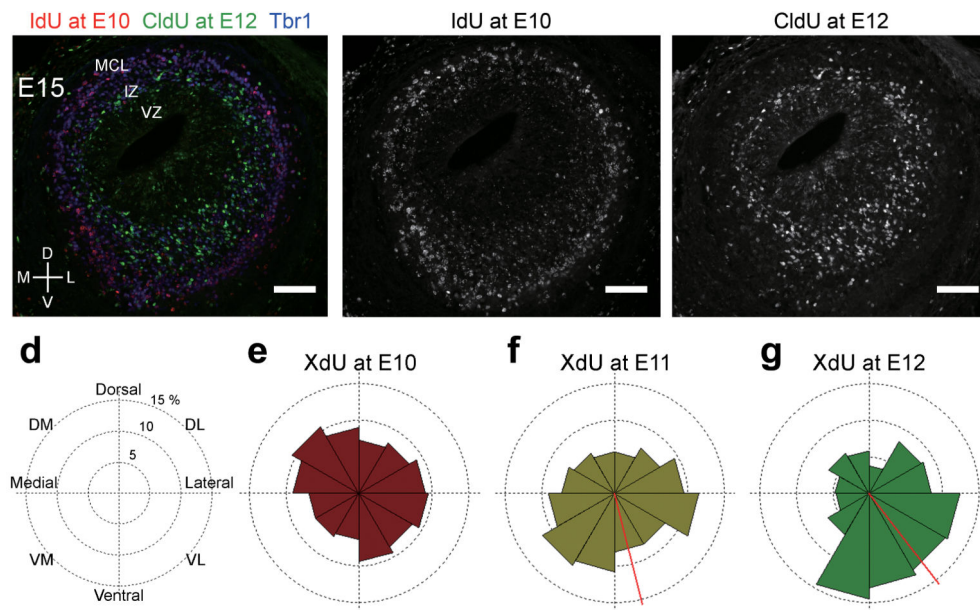


Figure 2.

Preferential integration of late-generated mitral cells into the ventrolateral portion of the developing olfactory bulb.

(a–c) A coronal section of E15 olfactory bulb immunostained with IdU (red), CldU (green) and Tbr1 (blue) (a). IdU (b) and CldU (c) were injected into pregnant dam at E10 and E12, respectively. E10-generated mitral cells non-preferentially distribute within the MCL, while E12-generated mitral cells are preferentially localized at the ventrolateral portion; IZ: intermediate zone; VZ: ventricular zone. (d–g) Quantification of distribution of Tbr1+ cells generated at E10 (e), E11 (f), or E12 (g) in E15 olfactory bulb. Thymidine analogs (XdU) were injected at each time point. Six olfactory bulb sections (3 animals) were analyzed for each time points of generation. Each olfactory bulb section was radially-separated into twelve compartments (d), and the percentages of XdU+/Tbr1+ cells found in each compartment among total XdU+/Tbr1+ cells in the section are shown with rose graphs (e–g). A non-uniform distribution around the circle is found with E11- ($p < 0.001$) and E12-generated mitral cells ($p < 0.001$), but not with E10-generated mitral cells ($p = 0.258$) (Rayleigh test). The population mean angle is shown with red bar in the graph only when non-uniform distribution around circle is found with Rayleigh test. Both E11- ($p < 0.001$) and E12-generated mitral cells ($p < 0.001$) preferentially distributed around the population mean angles (V-test, a modified Rayleigh test). Scale bars represent 100 μm .

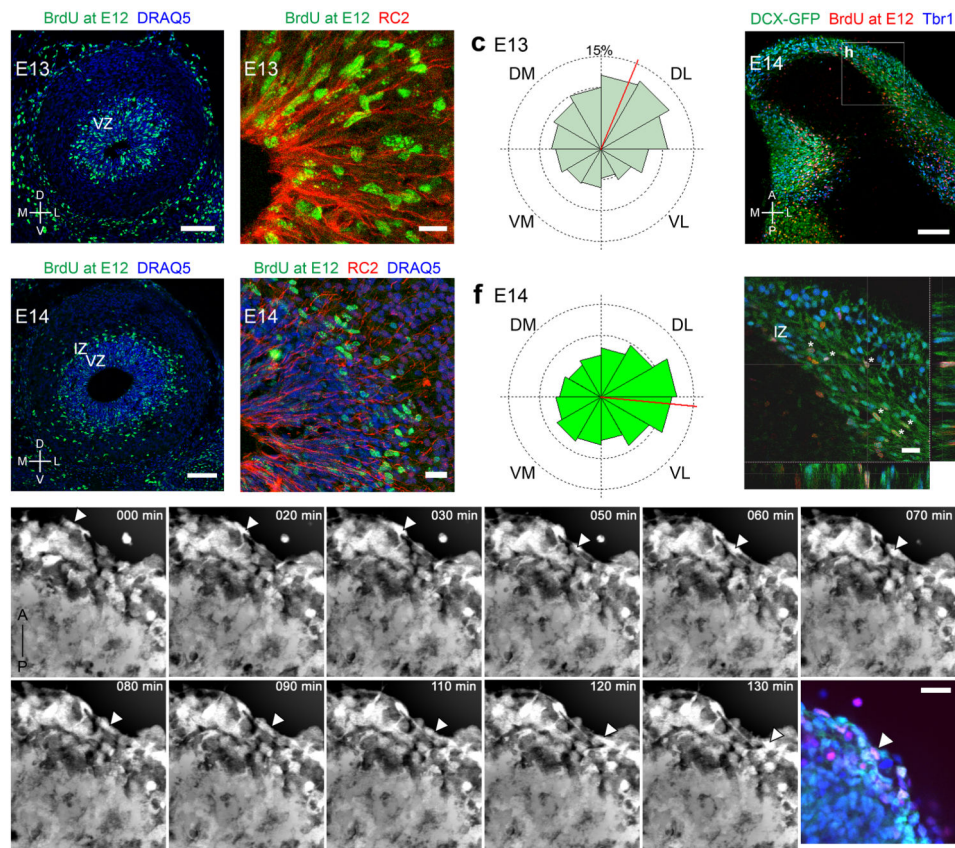


Figure 3.

Tangential migration of late-generated mitral cells in the developing olfactory bulb.

(a,b,d,e) Coronal sections of E13 (a,b) and E14 (d,e) olfactory bulbs in which E12-generated cells were labeled with BrdU (green). Radial glial processes were immunostained with RC2 (b,e; red). (c,f) Quantification of BrdU+ cell distributions in E13 (c) and E14 (f) olfactory bulb sections with the method described in Figure 2d. A non-uniform distribution of E12-generated cells was found at both E13 ($p < 0.001$; $n = 6$ olfactory bulbs) and E14 ($p < 0.001$; $n = 6$) (Rayleigh test). The population mean angle (red bar) is seen in dorsolateral region at E13, while it is shifted to lateral region at E14. At both E13 ($p < 0.001$) and E14 ($p < 0.001$), E12-generated cells were preferentially distributed around the population mean angles (V-test). (g,h) Horizontal section of E14 DCX-GFP mouse olfactory bulb immunostained with BrdU (red) and Tbr1 (blue). BrdU labels E12-generated cells. GFP+ cells in the intermediate zone have a tangentially elongated morphology. BrdU+ or Tbr1+ cells are mostly GFP+, and triple-labeled cells are also found in the slice (h). (i) Time-lapse imaging of acute DCX-GFP E14 mouse olfactory bulb slice was carried out to determine the mode of migration of GFP+ cells. A z-stack projection was prepared to track cell movement in different planes. The arrows show the progression of a GFP+ cell toward the posterior portion of the olfactory bulb. (j) A single optical slice shows that the GFP+ cell observed in (i) expresses Tbr1 (red). Scale bars represent $100\mu\text{m}$ (a,d,g) and $20\mu\text{m}$ (b,e,h,j).

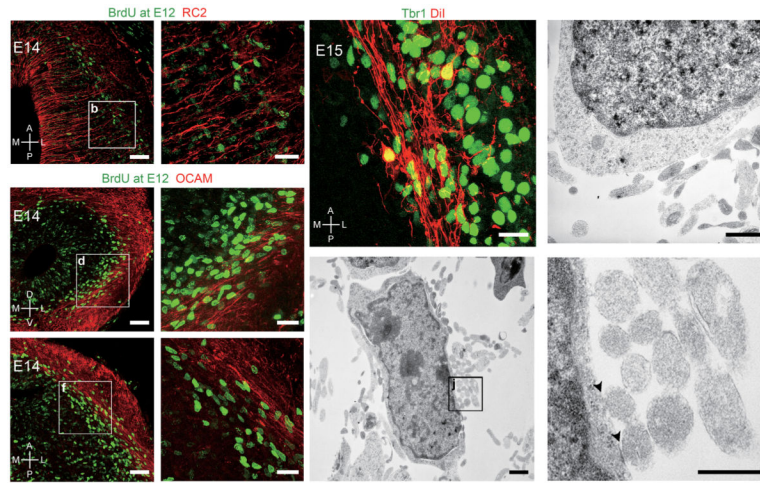


Figure 4.

Direct contact of E12-generated mitral cells with pre-existing mitral cell axons.

(a,b) Horizontal section of an E14 olfactory bulb immunostained with BrdU (green, E12-generated cells) and RC2 (red). RC2+ processes do not run tangentially in the olfactory bulb. (c–f) Coronal (c,d) and horizontal (e,f) sections of E14 olfactory bulb immunostained with BrdU (green, E12-generated cells) and OCAM (red) that labels mitral cell axons. Mitral cell axons run tangentially in the intermediate zone and contact tangentially elongated BrdU+ cells. (g) Horizontal section of an E15 olfactory bulb. Mitral cell axons were labeled with DiI (red) injected into lateral olfactory tract, and the nuclei of mitral cells were immunostained with Tbr1 (green). Pre-existing mitral cell axons pass the intermediate zone where many mitral cells that have a tangentially elongated morphology are found. (h–j) Electron microscopic images taken from E15 olfactory bulbs. Electron dense products were produced in nuclei of Tbr1+ cells with a DAB reaction. Tbr1+ cells with elongated nuclei are surrounded by many axons (h,i), and some axons make direct contacts with Tbr1+ cells (j; arrowheads). Scale bars represent 50 μ m (a,c,e), 20 μ m (b,d,f,g), 1 μ m (h,i), and 500nm (j).

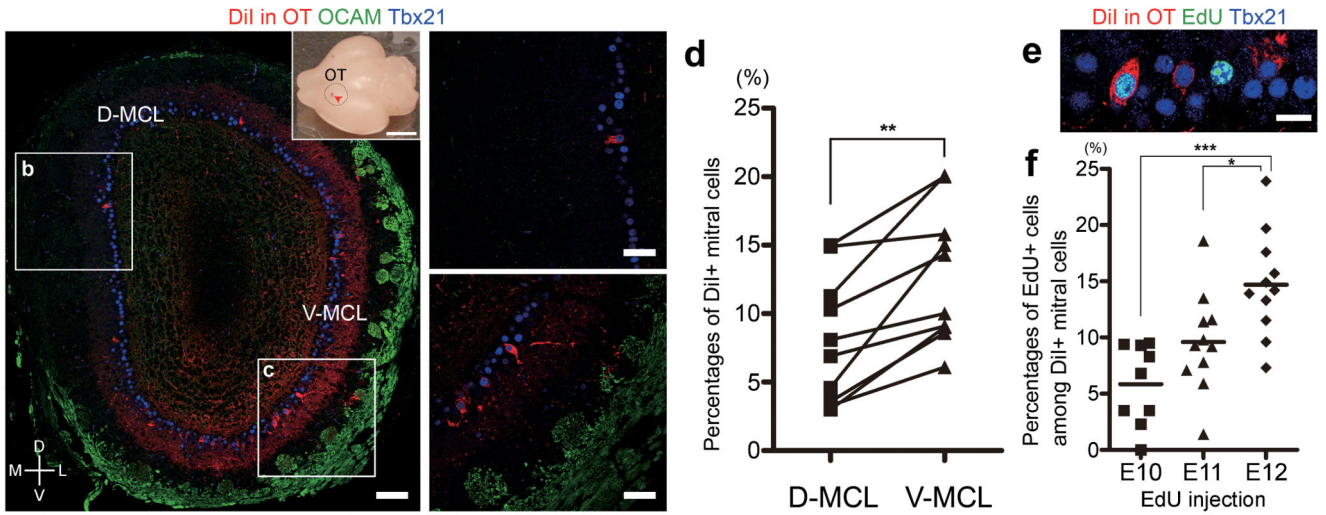


Figure 5.

Birthdate-regulated axonal projection to the olfactory tubercle.

(a–c) A coronal section of P5 olfactory bulb. A subpopulation of mitral cells was labeled with DiI injected into the olfactory tubercle. The injection site is shown with arrowhead in the inset. Many DiI+ (red) mitral cells (Tbx21+; blue) are found in the ventrolateral portion (c), while fewer DiI+ mitral cells are in the dorsomedial portion (b). (d) The MCL in olfactory bulb sections was subdivided into D- and V-MCLs based on the OCAM expression pattern in the glomerular layer (green in (a)), and the percentages of DiI+ mitral cells were quantified in each zone. A significantly higher percentage of V-MCL mitral cells were DiI+ than in the D-MCL (** $p=0.002$; $n=10$ olfactory bulbs; Wilcoxon signed rank test). (e) Detection of olfactory tubercle projecting mitral cells generated at specific time points in development. EdU injected at E12 was detected (green) in mitral cells (Tbx21+; blue) after DiI (red) injection into the olfactory tubercle at P5. (f) Percentages of EdU+ cells among olfactory tubercle projecting (DiI+) mitral cells were quantified after injecting EdU at E10, E11, or E12. The percentage is higher with EdU injection at E12 ($n=11$ olfactory bulbs) than E10 ($n=9$) and E11 ($n=11$) injection. * $p<0.05$; *** $p<0.001$; one-way ANOVA followed by Tukey's multiple comparison test. Scale bars represent 100 μm (a), 2mm (inset in a), 50 μm (b,c), and 20 μm (e).